Atmos. Meas. Tech., 7, 3373–3386, 2014
www.atmos-meas-tech.net/7/3373/2014/
doi:10.5194/amt-7-3373-2014

Atmospheric Measurement Techniques
Open Access

Long-path averaged mixing ratios of O_3 and NO_2 in the free troposphere from mountain MAX-DOAS

L. Gomez[1,2], M. Navarro-Comas[1], O. Puentedura[1], Y. Gonzalez[3], E. Cuevas[3], and M. Gil-Ojeda[1]

[1]Instituto Nacional de Técnica Aeroespacial (INTA), Área de Investigación e Instrumentación Atmosférica, Ctra Ajalvir km4, 28850, Torrejón de Ardoz, Madrid, Spain
[2]Groupe de Spectrométrie Moléculaire et Atmosphérique, URM CNRS 7331, UFR Sciences Exactes et Naturelles, Moulin de la Housse, BP 1039, 51687 Reims CEDEX 2, France
[3]Centro de Investigación Atmosférica de Izaña (Agencia Estatal de Meteorología –AEMET), Santa Cruz de Tenerife, Spain

Correspondence to: L. Gomez (lauragm.madrid@gmail.com)

Received: 7 May 2013 – Published in Atmos. Meas. Tech. Discuss.: 5 September 2013
Revised: 28 August 2014 – Accepted: 29 August 2014 – Published: 7 October 2014

Abstract. A new approximation is proposed to estimate O_3 and NO_2 mixing ratios in the northern subtropical free troposphere (FT). The proposed method uses O_4 slant column densities (SCDs) at horizontal and near-zenith geometries to estimate a station-level differential path. The modified geometrical approach (MGA) is a simple method that takes advantage of a very long horizontal path to retrieve mixing ratios in the range of a few pptv. The methodology is presented, and the possible limitations are discussed. Multi-axis differential optical absorption spectroscopy (MAX-DOAS) high-mountain measurements recorded at the Izaña observatory (28°18′ N, 16°29′ W) are used in this study. The results show that under low aerosol loading, O_3 and NO_2 mixing ratios can be retrieved even at very low concentrations. The obtained mixing ratios are compared with those provided by in situ instrumentation at the observatory. The MGA reproduces the O_3 mixing ratio measured by the in situ instrumentation with a difference of 28 %. The different air masses scanned by each instrument are identified as a cause of the discrepancy between the O_3 observed by MAX-DOAS and the in situ measurements. The NO_2 is in the range of 20–40 ppt, which is below the detection limit of the in situ instrumentation, but it is in agreement with measurements from previous studies for similar conditions.

1 Introduction

The knowledge of reactive trace gas distributions in populated areas around the world has greatly improved recently due to the extensive deployment of measurement networks on local to regional scales. Field instrumentation generally provides information on the surface concentrations, rather than the vertical distributions, of the measured species. As a consequence, knowledge of free troposphere (FT) tracer distributions is lacking. Recently, remote sensing instrumentation based on spectroscopic analysis Multi-axis differential optical absorption spectroscopy (MAX-DOAS) has demonstrated success in obtaining profiles in polluted areas and has been used extensively for pollution studies (i.e. Baidar et al., 2013; Hendrick et al., 2014) and satellite validation purposes (Peters et al., 2012; Ma et al., 2013). The use of MAX-DOAS has been essentially restricted to the boundary layer (BL) where most of the pollutants are located. Under stable conditions, a BL thermal inversion limits the upward ventilation of pollutants and other surface-produced tracers; as a result, the FT concentrations of gases such as NO_2 are much lower (possibly by orders of magnitude). Occasionally, due to favourable weather conditions or to mechanical forcing on given orographies, polluted air masses may be injected into the FT (Thakur et al., 1999).

The knowledge of tracers in the FT is relevant to determine atmospheric reference background conditions for pollution studies (Engardt et al., 2009; Beelen et al., 2009) and to study chemical processes occurring during long-range

transport (Thakur et al., 1999). Pollutants can be transported over long distances through the FT where fast winds exist and the lifetime of minor species is longer than that in the BL (Stohl and Trickl, 1999; Stohl et al., 2003; Liang et al., 2004). Unfortunately, little is known of the amounts of BL active species in the FT that are anthropogenically produced (Wenig et al., 2003); the downward exchange between the FT and the lower troposphere is also unclear (Zyryanov et al., 2012).

Routine measurements of background levels of chemically active trace gases in the FT are very scarce. FT measurements have been recorded during limited time periods on airborne platforms with high-quality instrumentation (Robinson et al., 2005; Mao et al., 2006; Martin et al., 2006; Oltmans et al., 1996; Thompson et al., 2011; Baidar et al., 2013), but the high cost of the flights prevents their use for long-term studies. Continuous monitoring programmes have been limited to the use of in situ instruments located in the few existing mountain observatories around the world. However, the measurements provided by these instruments are local and are usually affected by the so-called "mountain breeze effect" (MBE) (e.g. Cuevas et al., 1992; Reidmiller et al., 2010). Therefore, these measurements are not representative of the background conditions.

Here, we present results of data that are representative of the FT using the MAX-DOAS remote sensing technique at the Izaña station, a high-mountain observatory located in the Canary Islands in the Subtropical Atlantic Ocean. Unlike in situ measurements, MAX-DOAS integrates optical paths over a few tens of kilometres. As a result, inhomogeneities are averaged in the path, which in turn minimises the impact of the small-scale upwelling of air masses from the BL. Measurements can be recorded continuously as long as diffuse sunlight is available; the best results of the proposed method are provided at solar zenith angles (SZAs) up to 70°, as discussed in Sect. 3.

Using the MAX-DOAS technique, the slant column density (SCD) of a given gas is measured, i.e. the amount of gas along a given line of sight. To remove the dependence of the observation angle from the data, the SCD is converted to the vertical column density (VCD) using a conversion factor known as the air mass factor (AMF). The AMF, which can be calculated from radiative transfer models (RTMs), is closely related to the effective optical path (EOP), which is a single path that is equivalent to all ray paths that contribute to the measurement. The EOP is needed to obtain the density at a given altitude; it can be calculated using various approaches. The simplest one was introduced by Hönninger (Hönninger and Platt, 2002; Hönninger et al., 2004). This approach only considers single scattering and does not take into account surface albedo or aerosol extinction. More realistic methods consist of using RTMs together with the optimal estimation method (OEM) (Rodgers, 2000; Steck, 2002). These methods are similar and are computationally very costly. Later, Sinreich et al. (2013) presented a new method to obtain concentrations of trace gases in the BL. The method can be applied when light paths for the lowest elevation angles do not differ significantly, which is a consequence of the high aerosol loading in the atmosphere. The optical path is then obtained from the differential SCD (DSCD) of the O_4 (Wagner et al., 2004; Sinreich et al., 2005; Frieß et al., 2006; Clémer et al., 2010), which is the difference between the SCD at low instrumental elevation angles (IEAs) and the zenith SCD. However, if the aerosol load is too high, scattering at all elevations (high and low) occurs close to the detector, which leads to a poor performance of the model. Sinreich et al. (2010) and Mahajan et al. (2012) use a similar approximation for their studies in the marine boundary layer (MBL).

In general, the different approximations used to obtain tracer concentrations from MAX-DOAS measurements require multiple scattering mode in the radiative transfer calculations due to the (a) high air density, (b) large concentrations of pollutants and often water vapour, and (c) high aerosol loading. Here, we propose a modified version of the MAX-DOAS geometric approximation (Hönninger et al., 2004) to estimate FT tracer mixing ratios at very low concentrations. In particular, at the Izaña observatory, where the air density is low and the atmosphere is extremely clear, single scattering can be used. Aerosols are not considered here, thus assumptions on the aerosol vertical distribution and properties are not necessary, and therefore uncertainties related to the aerosols are avoided. This new method, which we call the "modified geometrical approach", takes advantage of the possibility of horizontal measurements to obtain gas mixing ratios, which provides a straightforward inversion. Here, the horizontal optical path is considered to be the difference between the optical paths of the zenith and horizon views; it is calculated using two procedures. The first procedure, called O_4-MGA (modified geometrical approach), uses the O_2 dimer (hereafter referred to as O_4) measurements at the level of the station. The second procedure, called RTM-MGA, uses a RTM to obtain the required paths. This method is valid for a single-scattering atmosphere and for scattering that occurs very close to the detector. Similar assumptions have been considered in some airborne MAX-DOAS studies (Melamed et al., 2003; Baidar et al., 2013) for nadir observations. In Baidar et al. (2013), all the photons are assumed to be scattered only once (single scattering) very close to the ground or reflected from the surface before they reach the airborne detector. In that study, the validity of these assumptions was confirmed. Here, the MGA is applied to estimate the O_3 and NO_2 concentrations at the Izaña observatory, where the required conditions are satisfied. The results are then compared with in situ measurements of both species. Because in situ measurements are based on different techniques/principles than DOAS (UV absorption cell for O_3 and chemiluminescence for NO_2), they are an independent and excellent set of measurements to validate the consistency of our method. The MGA can also be extended to other species

with structured absorption spectra in the near-UV and visible ranges, such as H_2O, HCHO, CHOCHO and IO.

This paper is organised as follows: in Sect. 2, the station and meteorology of the area are presented. In Sect. 3, the methodology is described and the assumptions and limitations are discussed. Sections 4 and 5 address the instrumentation and data. The results and discussion are provided in Sect. 6. Finally, the main conclusions are summarised in Sect. 7.

2 Izaña station

The Izaña Atmospheric observatory (28°18′ N, 16°29′ W) is located in Tenerife (Canary Islands) at an altitude of 2373 m a.s.l. This observatory is part of the Global Atmospheric Watch (GAW) programme and is managed by the Centro de Investigación Atmosférica de Izaña (CIAI) of the Agencia Estatal de Meteorología (AEMET, Spain). In the Canary Islands, the influence of the descending branch of the Hadley cell creates a high stability regime in the FT, whereas quasi-permanent NNE trade winds blow in the MBL (Palmén and Newton, 1969). The FT and MBL are well differentiated by a quasi-permanent strong temperature inversion that ranges between 800 and 1500 m a.s.l. (Font, 1956; Milford et al., 2008). The temperature inversion defines an upper limit to the MBL, which prevents pollution of the lower levels from reaching the FT. Therefore, the Izaña station is located well above the MBL and, during the night, is representative of the FT conditions. Below the station, at the base of the inversion, a layer of clouds is present on most days at the north side of the island. The clouds form as a result of the condensation of the humid air masses that are forced to ascend by the trade winds that arrive at the north face of the island. The Canary Archipelago is under the influence of a subtropical high-pressure system, which provides many days with a clear sky above the cloud layer.

The strong temperature inversion defines a discontinuity in the vertical distribution of gases, such as H_2O, NO_2 and O_3. During the night, subsiding air increases the O_3 and reduces the H_2O and NO_2; the opposite is true during the day. In particular, humid MBL air masses that move upslope due to the diurnal mountain breeze can reach the observatory; thus, typically, H_2O increases by 60 % and the NO_2 increases a few hundred ppt at the level of the station. In contrast, the O_3 suffers a decrease of 6.5 % (Cuevas et al., 1992; Puentedura et al., 2012). These variations in concentrations can be used as signatures of the origin of the air masses over the station. As for gases, the strong temperature inversion prevents sea salt and other aerosols below from reaching the observatory. Two typical situations occur at Izaña: very clean days with an aerosol optical depth (AOD) below 0.05 at 500 nm or Saharan dust days in which the AOD can reach values larger than 1 when Saharan dust transported from North Africa arrives at the island.

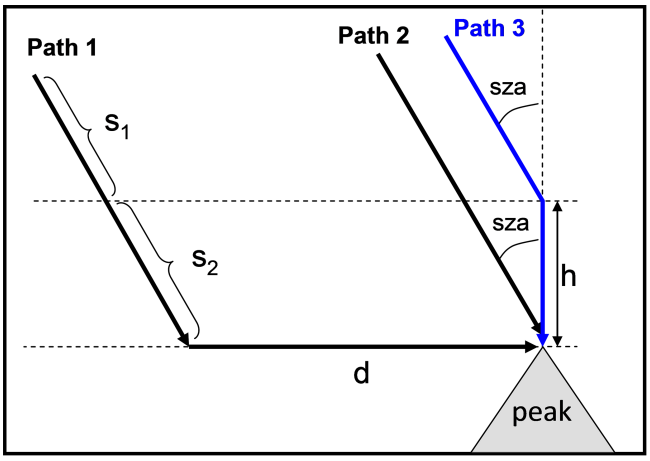

Figure 1. Schematic representation of a simplified optical path of scattered solar radiation for real (blue) and MGA-approximated (black) geometries.

3 Modified geometrical approach (MGA)

3.1 Methodology

The MGA is an extremely simple concept. It assumes a single-scattering geometry and a scattering point altitude close to the instrument. Under these simplified conditions, the column of the gas under consideration in the horizontal path (d in Fig. 1) is the differential column between zenith (IEA = 90°) and horizontal (IEA = 0°) measurements simultaneously obtained, because the slant paths are identical in both cases and cancel out. Alternatively, the zenith measurement can be used as a reference to evaluate the horizontal measurement; then, the outcome of the evaluation is directly the gas in the horizontal path. Therefore, the concentration of the gas x at the level of the station, $c_{x,\mathrm{st}}$, can be obtained simply from the difference of both slant columns divided by the length of the horizontal path (d):

$$c_{x,\mathrm{St}} = \frac{\mathrm{SCD}_{\mathrm{horiz},x} - \mathrm{SCD}_{\mathrm{vert},x}}{d}, \quad (1)$$

where $\mathrm{SCD}_{\mathrm{horiz},x}$ and $\mathrm{SCD}_{\mathrm{vert},x}$ are the slant columns in the horizontal and vertical views, respectively. If measurements are not simultaneously taken, then $\mathrm{SCD}_{\mathrm{vert},x}$ has to be multiplied by a correction factor f to reference them to the same SZA, which is defined as

$$f = \mathrm{AMF}(\mathrm{sza}_1)/\mathrm{AMF}(\mathrm{sza}_2), \quad (2)$$

where AMF is a factor of the zenith geometry (IEA = 90°) and sza_1 and sza_2 are the solar zenith angles at the times of the horizontal (IEA = 0°) and vertical (IEA = 90°) measurements.

Within the MGA, two different methods have been considered to estimate d: O_4-MGA and RTM-MGA. The first method obtains d from the SCD of O_4 (SCD_{O_4}), which is

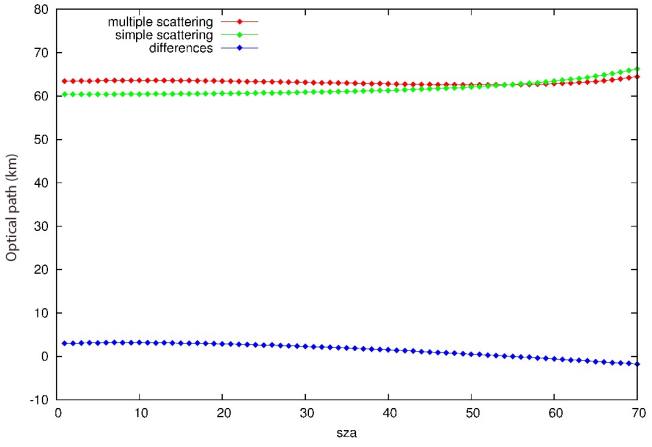

Figure 2. Horizontal optical paths obtained from the SPDISORT solver when single (green diamonds) and multiple (red diamonds) scattering are considered. The blue diamonds correspond to the differences between the single and multiple scattering paths.

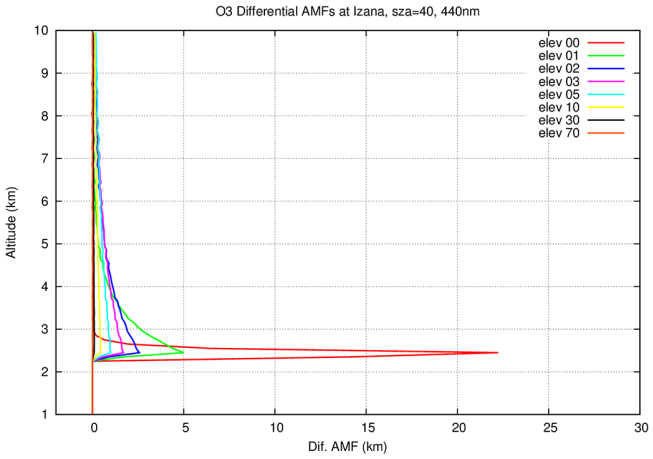

Figure 3. Differential box-AMFs (with respect to the zenith) for the Izaña observatory. The calculations were performed at 440 nm.

measured simultaneously with the gases in which the concentration is to be retrieved and with the monthly mean oxygen concentration (c_{O_2}) at the level of the station. An advantage of the method is that no RTMs are needed:

$$d = \frac{\mathrm{SCD}_{\mathrm{horiz,O_4}} - \mathrm{SCD}_{\mathrm{vert,O_4}}}{(c_{O_2})^2}. \quad (3)$$

In the second method (RTM-MGA), the horizontal paths for each geometry (d') are obtained from the radiative transfer model (at sza_1). Then, the gas concentration can be estimated in a similar manner as in Eq. (1):

$$c'_{x,\mathrm{St}} = \frac{\mathrm{SCD}_{\mathrm{horiz},x} - \mathrm{SCD}_{\mathrm{vert},x}}{d'}. \quad (4)$$

The radiative transfer model used in this paper does not directly supply the optical path. In this case, the following equation is used for the calculation of d':

$$d' = \frac{\mathrm{SCD}_{\mathrm{horiz},x} - \mathrm{SCD}_{\mathrm{vert},x}}{c_x}, \quad (5)$$

where x refers to O_3 or NO_2. In this case, the concentration of these species, c_x, at the level of the station is obtained from the Air Force Geophysics Laboratory (AFGL) standard atmosphere for tropical latitudes (Anderson, 1986).

The first assumption required for the validity of the MGA is a single scattering atmosphere. To estimate the adequacy of this approximation for the conditions given in this research, the horizontal optical paths as a function of the SZA for single and multiple scattering are calculated for the Izaña observatory conditions. The SDISORT radiative transfer model (Dahlback and Stamnes, 1991) is used to obtain these horizontal paths from O_4 SCDs. The inputs of these calculations are summarised in Table 2. The results are shown in Fig. 2. The differences for the SZAs that are lower than or equal to 70° are as high as 5 %. These results confirm that in the pristine Izaña atmosphere, single scattering can be used.

The MGA is also based on the assumption that when evaluating a spectrum in the horizontal direction (elevation = 0°) using the zenith spectrum as a reference, the vertical components cancel out. To prove that this is true for the conditions of this research, we use the SDISORT radiative transfer model (Dahlback and Stamnes, 1991) to calculate the single-scattering O_3 differential box-AMFs defined as

$$\mathrm{DiffAMF} = [\mathrm{AMF}(\alpha) - \mathrm{AMF}(90)]\Delta z, \quad (6)$$

where α is a given elevation angle, and Δz is the thickness of the layers of constant concentration considered in the radiative transfer model (100 m in this case). This magnitude provides the difference of the optical paths for both elevation angles (0 and 90°) for each of these layers. The results are shown in Fig. 3 for an SZA = 40°. For an elevation angle = 0°, the differential box-AMF is the maximum at the level of the station but becomes zero near an altitude of 3 km and higher, which is only 0.6 km above the station. Similar results are observed for other SZAs, except for twilight (SZA > 70°), for which the method is not applicable (shown later). This result proves that the slant contribution (before the scattering point) of the paths at IEAs of 0 and 90° cancel out and that only the horizontal path remains.

3.2 Error estimation

The error in the concentration using Eq. (1) depends on the measurements (SCD of the considered gas) and the path errors. The average measurement relative error for typical values of NO_2 and O_3 and their corresponding molecular errors – as defined in Platt and Stutz, 2008 (using mean values during 2011 to 2013 at Izaña) – are 23 and 6 %, respectively. However, the path error depends on the O_4 SCD fitting error (approximately 0.1 % and negligible), the air density error

(lower than 2 % at Izaña in summer) and the cross-section error. Major uncertainties stem from a potential bias of the O_4 cross-sections (Wagner et al., 2002, 2009; Clemer et al., 2010); nevertheless, they are under debate. If only the air density error is considered, the path error following Eq. (3) is approximately 4 %. Taking into account all these values, the typical relative errors of the NO_2 and O_3 concentrations are 23.3 and 7.4 %, respectively.

The estimation of the error of the concentrations obtained from this method must also be considered. Actually, the scattering occurs at a certain height h above the station. The blue line in Fig. 1 represents the EOP, which is defined as the geometrical ray equivalent to the zenith integrated flux at the station. Accordingly, h is the "effective" scattering height. In this more realistic geometry, the difference between the horizontal and vertical measurements is

$$\begin{aligned} \mathrm{SCD}_{\mathrm{horiz}} - \mathrm{SCD}_{\mathrm{vert}} &\equiv \mathrm{SCD}_{\Delta} \\ &= (S_1 + S_2 + D) - (S_1 + H) \\ &= D + H\,(\mathrm{AMF(sza)} - 1)\,, \end{aligned} \tag{7}$$

where S_1, S_2, D and H are gas partial columns along the considered paths s_1, s_2, d and h, respectively, and $\mathrm{AMF(sza)} = S_2/H$. If

$$g = \mathrm{AMF(sza)} - 1, \tag{8}$$

then

$$D = \mathrm{SCD}_{\Delta} - gH. \tag{9}$$

The second term in the right-hand side of the equation is the overestimation factor. Both parameters, g and H, are SZA dependent.

The relative error can be given as

$$\varepsilon = \frac{gH}{dc_{x,\mathrm{st}}} = \frac{gh\bar{c}_x}{dc_{x,\mathrm{st}}} = \frac{ghR}{d}, \tag{10}$$

where $\bar{c}_x$ is the mean concentration in the layer between the station and the scattering altitude, which can be written as a fraction R of the concentration at the level of the station, $c_{x,\mathrm{st}}$.

To estimate the relative error versus the SZA, the scattering height h must be calculated. Let $I(z)$ be the contribution of the flux scattered at level z to the total flux at the surface. We define a weighed intensity (WI) as

$$\mathrm{WI}(z) = \frac{I(z)}{\int I(z)\mathrm{d}z}. \tag{11}$$

For a given SZA, WI represents a normalised contribution of the ray I scattered at level z to the total flux observed at the station (Solomon et al., 1987), and can be calculated with RTMs. Then, h is

$$h = \frac{\sum_{\mathrm{station}}^{\mathrm{TOA}} (\mathrm{WI}(z) \cdot z)}{\sum_{\mathrm{station}}^{\mathrm{TOA}} \mathrm{WI}(z)}. \tag{12}$$

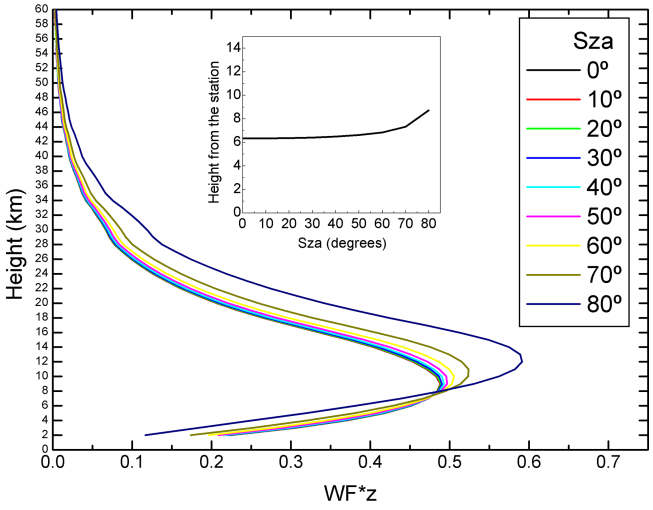

Figure 4. Scattering height versus weighted intensity times the altitude for different SZAs.

Figure 4 shows that h is nearly constant up to an SZA of 70–75°. However, g increases exponentially towards large SZAs.

If the length of the horizontal path d is obtained with the help of the O_4, which is retrieved simultaneously with the NO_2 and O_3 columns (Eq. 3), then the O_4 path is also overestimated. The actual concentration of the gas x at the level of the station is

$$c_{x,\mathrm{st}} = \frac{\mathrm{SCD}_{\Delta,x} - gH}{d} = (c_{\mathrm{O_2,st}})^2 \frac{\mathrm{SCD}_{\Delta,x} - gh\bar{c}_x}{\mathrm{SCD}_{\Delta,\mathrm{O_4}} - g'h\bar{c}_{\mathrm{O_4}}}. \tag{13}$$

The second terms above and below the fraction bar are the correction factors. $\bar{c}_x$ and $\bar{c}_{\mathrm{O_4}}$ are the mean concentrations in the layer between the station and the scattering altitude, which can be written as fractions, R and R', of the concentrations at the level of the station:

$$c_{x,\mathrm{st}} = (c_{\mathrm{O_2,st}})^2 \frac{\mathrm{SCD}_{\Delta,x} - ghRc_{x,\mathrm{st}}}{\mathrm{SCD}_{\Delta,\mathrm{O_4}} - g'hR'(c_{\mathrm{O_2,st}})^2}, \tag{14}$$

which, with reassigning, yields

$$c_{x,\mathrm{st}} = \frac{\mathrm{SCD}_{\Delta,x}}{\frac{\mathrm{SCD}_{\Delta,\mathrm{O_4}}}{(c_{\mathrm{O_2,st}})^2 + h(Rg - R'g')}}. \tag{15}$$

The error in the path, the term $h(Rg - R'g')$, depends on the vertical distribution of the tracer under consideration and the differences in the AMF between the tracer and the O_4. If the vertical distribution does not vary much with height, we can estimate the error as differences in the AMF. Figure 5 shows the relative error in O_3 and NO_2 assuming a horizontal path of 60 km (approx. $\mathrm{AOD}_{500\ \mathrm{nm}} = 0.02$) and a constant vertical volume mixing ratio (VMR). As observed, the best results of the MGA are obtained for SZAs up to 70°.

Note that the observed errors do not increase if a moderate amount of aerosols are present ($\mathrm{AOD}_{500\ \mathrm{nm}} = 0.1$) because both the numerator and denominator in Eq. (15) are reduced by approximately the same ratio.

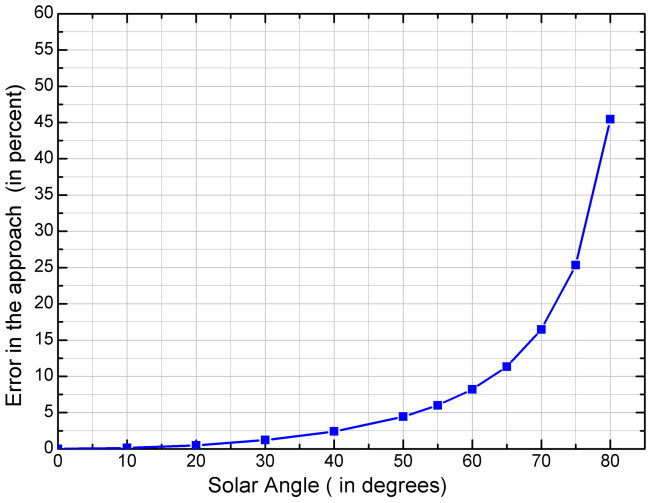

Figure 5. Estimated error of the MGA versus the SZA.

4 MAX-DOAS measurements and data

MAX-DOAS measurements were recorded at a terrace on the Izaña station using an INTA spectrometer, the RASAS-II, in the summer of 2011. In Table 1, the instrument settings are summarised. Further details can be found in Roscoe et al. (2010) and Puentedura et al. (2012). Note that the field of view of the light collector was narrowed (with respect to previous studies) to 1°, which reduced the uncertainties of the scanned air masses. Most of the instrument-collected radiation originated from the FT (Puentedura et al., 2012), and the largest contribution was from the station level. RASAS-II is pointed north and collects scattered radiation from several elevation angles between −1 and 90°. However, because the sun is directly overhead at noon during the subtropical summer, the zenith data were not collected at that time to avoid damage due to direct sunlight on the detector. Data at IEA = 70° are instead used in our calculations. Consequently, SCD_{vert} in the equations corresponds to $\alpha = 70°$ instead of 90°. The impact of this change was tested and found to be negligible.

Spectra recorded by RASAS-II were processed to obtain the SCDs of O_3, O_4 and NO_2. This retrieval was performed using a code developed at INTA (Gil et al., 2008) based on the standard DOAS technique (Platt and Stutz, 2008). In the present analysis, a spectral range from 430 to 500 nm was chosen. This range differs from that suggested by the Network for the Detection of Atmospheric Composition Change (NDACC) for O_3 [450–550 nm]. An extension to 430 nm was chosen to perform a single NO_2 and O_3 analysis that covers the large O_4 477 nm absorption. The longest wavelengths were truncated to avoid the strong H_2O absorption band at 500–510 nm. H_2O bands cannot be accurately fitted because the effective absorption cross sections are dependent on the actual H_2O concentration due to saturation (Clémer et al., 2010). Although the truncation of the spectral upper range at 500 nm improves the fitting, an inspection of the remaining residuals clearly shows systematic structures in the flanks of the water cross-sections' weak bands centred at ∼445 and ∼487 nm and the strong 477 nm O_4 band. The structures were removed using a pseudo-cross-section generated as the residual mean of 3 days of clear data (approx. 1000 spectra). Careful testing was performed to ensure that no interference occurred. The results had almost no impact on the retrieved amounts, and the stability of the IEA cycles (differences between the contiguous cycles) improved.

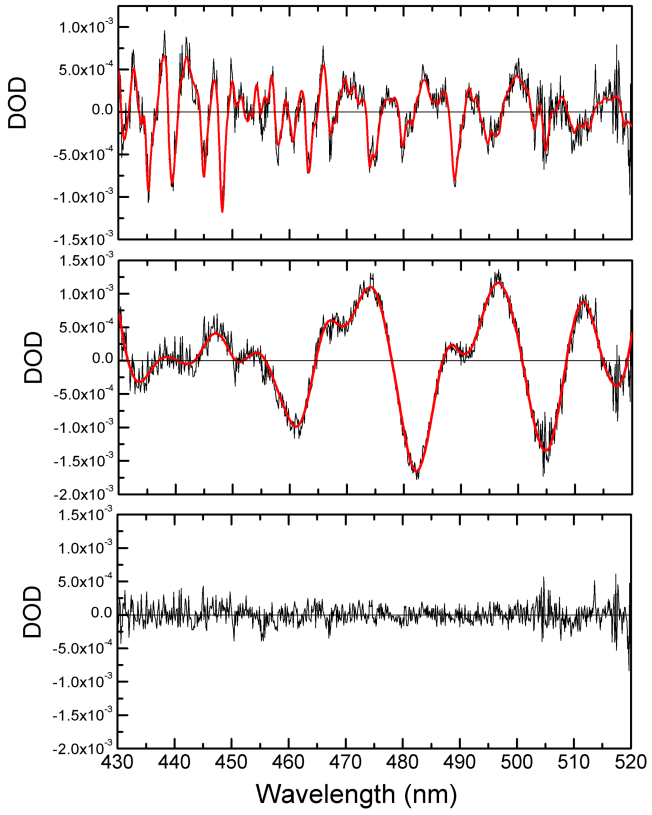

Figure 6. Example of a horizontal DOAS fit using a zenith spectrum as a reference. Values of 4.0×10^{15} and 8.7×10^{18} molecules cm^{-2} for NO_2 (upper panel) and O_3 (middle panel), respectively, were obtained during this cycle. The residual is shown in the lower panel.

Although the differential absorption signal between 70° and the horizon was small in the unpolluted FT, the measurements were of good quality. Following Platt and Stutz (2008), the typical instrumental detection limits (DL) for the measurements used in the present study were 4×10^{13} and 8×10^{16} molecules cm^{-2} for NO_2 and O_3, respectively, for the typical root mean square error of the residuals of a 2.5×10^{-4} differential optical depth (DOD). Assuming no error occurred in the optical path estimation, this DL was lower than 1 ppt for NO_2 and 1 ppb for O_3. As mentioned previously, the contribution of the fitting error of O_4 was negligible (0.1 %). Major uncertainties stem from the potential bias

Table 1. Instrumental characteristics and parameters used in the fit of the spectra.

Instrumental		
FWHM		0.52–0.58 nm
Linear dispersion		0.11 nm pixel^{-1}
F.O.V.		1°
Instrument elevation angles (IEAs)		90, 70, 30, 10, 5, 3, 2, 1, 0, −1°
Azimuth		Fixed to north
Time for collecting a single spectrum		From 0.2 s at noon to 10 s at 90° SZA
Time for a single measurement		Spectra co-added for 120 s
Time of a complete cycle		4 min
Fit parameters		
Spectral interval		430–500 nm
Orthogonalisation polynomial		3rd degree
Offset		Inverse of the reference
Reference spectrum		A single one for the entire period. At zenith and SZA = 70°
Absorption cross-sections		
Molecule	Temperature	Reference
O_3 ($I_0 = 10^{19}$ molec cm^{-2})	223 K	Bogumil et al. (2001)
NO_2 ($I_0 = 5 \times 10^{16}$ molec cm^{-2})	220 K	Vandaele et al. (1998)
H_2O	296 K	HITRAN update 2009 (Rothman et al., 2008)
O_4	298 K	Hermans et al. (1999)*
Rot. Raman Scatt. (Ring effect)		WINDOAS package (Fayt and Van Roozendael, 2001)

* Data can be found at http://spectrolab.aeronomie.be/o2.htm.

in the O_4 cross-sections (Wagner et al., 2002, 2009; Clémer et al., 2010) used to obtain the optical path. An example of the DOAS fitting is shown in Fig. 6, and the standard diurnal evolution of DSCDs of O_3, NO_2, O_4 and H_2O on a clear day for all IEAs is shown in Fig. 7. Note that NO_2 and O_3 DSCD plots have a u-shape due to their high concentration in the stratosphere. This signature is not observed in the DSCDs of O_4 because most of the oxygen resides in the troposphere.

5 In situ measurements

The performances of O_4-MGA and RTM-MGA were tested by comparing their estimated concentrations of O_3 and NO_2 with the in situ measurements available at the Izaña observatory. The NO_2 and O_3 in situ concentrations were measured with a chemiluminescence NO-NO_2-NO_X analyser (Model 42C-TL, Thermo Electron Corporation) and two UV photometric O_3 analysers running in parallel (Model 49C, Thermo Electron Corporation), respectively. Detection limits of these instruments are 50 ppt and 1 ppb, respectively. The sampled air masses were captured by two inlet systems on the top of the observation tower, which is located 4 m above the terrace. One of the inlets is used for the O_3 determination, and the second inlet is used for measuring the remaining tracers. A laminar vertical flux manifold ensures that the residence times of the air masses along the sample are smaller than 10 s. The quality control for ozone (Cuevas et al., 2013) includes a 15 min daily check of zeros, calibration of the O_3 analyser with a primary standard model 49C-PS, and quality audits periodically performed by the World Calibration Centre (WCC-EMPA). The calibration of the NO_2 analyser (González, 2012) is performed using a multi-gas calibrator and certified gas bottles provided by Air Liquide Inc. The Environmental Protection Agency of the United States (EPA) and the European Union have declared these measurement techniques as reference methodologies. Furthermore, these techniques fulfil the Global Atmospheric Watch Programme requirements.

The main drawback of the measurements provided by these instruments is that they are usually affected by the radiatively induced local circulation. During the day, the upslope wind transports tracers from the lower levels (MBE, e.g. Cuevas et al., 1992; Reidmiller et al., 2012), whereas at night, a quasi-permanent katabatic NW flow is normally present at the level of the station, except during Saharan air mass intrusions (Cuevas et al., 2013). As a result, only night-time in situ measurements are representative of FT conditions. The diurnal intensity of the MBE is modulated by insolation and the synoptic wind. The stronger the synoptic wind, the smaller the influence of the MBE (Cuevas et al., 2013).

Ozone sounding data of the NDACC programme are also available. Ozonesondes are launched on a weekly basis from the Orotava station (28°25′ N, 16°18′ W) in Puerto de la

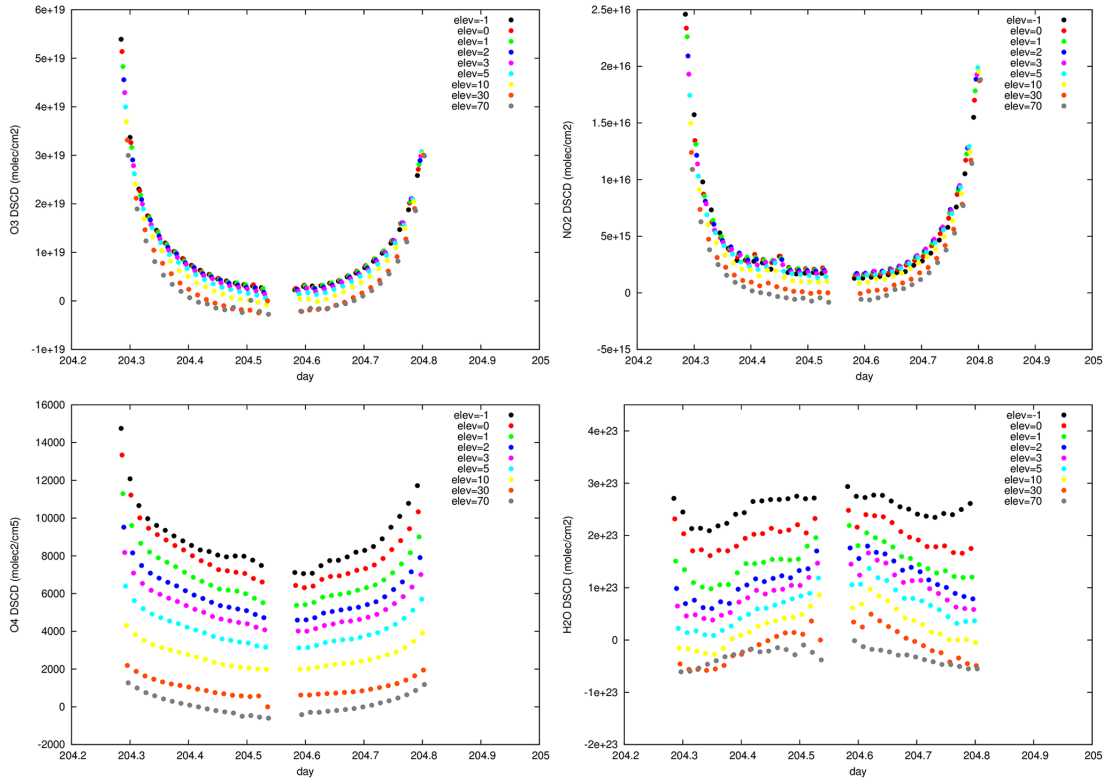

Figure 7. MAX-DOAS measured DSCD of O_3 (top left), NO_2 (top right), O_4 (bottom left) and H_2O (bottom right) for day 204 and for all elevation angles.

Cruz (Tenerife) at a horizontal distance of approximately 13 km from Izaña. Ozone soundings provide O_3 concentrations and meteorological data (pressure, temperature and humidity) from sea level to 30–35 km altitudes with a vertical resolution of 100–150 m (Cuevas et al., 1994). O_3 is measured by the standard ECC method (Thompson et al., 2011; Smit, 2011).

6 Results and discussion

The O_3 and NO_2 concentrations at the Izaña station were estimated using both O_4-MGA and RTM-MGA. To ensure that the assumptions of the approximation are met (single-scattering atmosphere and scattering close to the detector), only measurements at SZAs lower than 70° were used. Measurements taken on clear days (AOD below 0.05) were considered here. Figure 8 shows the AERONET level 2 (cloud-screened and calibrated data) AOD at 500 nm obtained by the CIMEL sun photometer over the station during July and the beginning of August 2011. Five well-identified Saharan events occurred during this period. The rest of the days exhibited clear skies with typical AODs below 0.05. In this period, we selected a set of 9 summer days (days 200–208 of 2011) in which the first 8 correspond to clear sky days. On

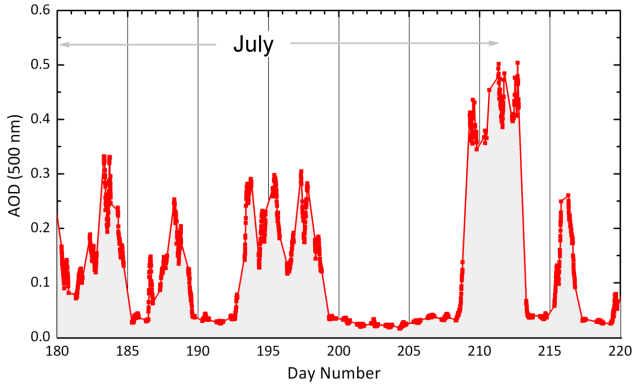

Figure 8. Integrated AOD at 500 nm obtained at the Izaña station on days 180–220 of 2011.

the last day, only the first hours were considered because Saharan dust arrived at the station in the early afternoon.

O_3, NO_2 and O_4 SCDs were simultaneously measured by the MAX-DOAS spectrometer. For the O_4-MGA, the path was directly obtained by Eq. (3). Because the pressure variation from one day to another is only 2 % in summer, the air

Table 2. Input parameters used in libRadtran for the optical path calculations.

LibRadtran inputs	
Atmosphere model	Standard atmosphere for tropical latitudes: afglt
Aerosols	No aerosols
Cloud	Optical depth 5, 0.6–1.1 km
Albedo	0.07
Instrument azimuth	Fixed to north
Solar azimuth	Variable
Solar zenith angle	From 0 to 70° in 1° intervals
Elevation angle	0.1 and 70°
Wavelength	440 nm (O_3 and NO_2), 477 nm (O_4)
Scattering	Single scattering
Cross-section (O_3)	Bogumil et al. (2001) (223 K)
Cross-section (NO_2)	Vandaele et al. (1998) (220 K)
Cross-section (O_4)	Greenblatt et al. (1990) (296 K)
Solver	SDISORT

density radiosonde monthly climatology was used to obtain the O_4 concentration at the level of the station.

Optical paths were also estimated from the radiances obtained by the pseudo-spherical discrete ordinate solver SDISORT (Dahlback and Stamnes, 1991) that is included in the software package libRadtran version 1.7 (Mayer and Kylling, 2005) for the RTM-MGA. This solver considers direct radiation in a spherical Earth framework and the scattering of light in a plane-parallel configuration. Vertical profiles of the gas densities were taken from the AFGL standard atmosphere for tropical latitudes (Anderson, 1986). Due to the low AOD found at the station for the selected days, no aerosols were considered in the simulations. Furthermore, to best reproduce the conditions of the site, a homogeneous cloud located between 600 and 1100 m a.s.l. was included in the model. The altitude values of the cloud top and base were estimated from the European Centre for Medium-Range Weather Forecasts (ECMWF) using summer conditions from 2008 to 2011 for 24 h forecasts computed at intervals of 6 h. These altitude values are consistent with the radio-soundings and present a small day-to-day variability during summer (J. J. Bustos, personal communication, 2010). Additionally, we used an optical depth of the cloud equal to 5 (at 500 nm), as catalogued by the International Satellite Cloud Climatology Project (ISCCP), and a standard marine surface albedo of 0.07. The instrumental azimuth is set to zero, and the solar azimuth dependence is considered in all of our calculations. The RTM calculations were performed at 440 nm for O_3 and NO_2. Under these conditions (summarised in Table 2), the values of the difference between the optical paths for the zenith and horizon views (d in the equations) were obtained for SZAs from 0 to 70° in intervals of 1°. To obtain intermediate values, linear interpolation was used.

6.1 Ozone concentration

In Fig. 9, the O_3 mixing ratios obtained using O_4-MGA (blue) and single-scattering RTM-MGA (red) are compared to the O_3 in situ measurements (black). The concentrations based on O_4-MGA yield diurnal evolutions similar to those obtained using RTM-MGA. The MGA captures the day-to-day variability well. However, the mean difference between the in situ and the MAX-DOAS values for the selected period was 28 %. In general, larger values are observed by MAX-DOAS. The possible causes of this discrepancy are described below.

The O_4-MGA relies on the accuracy of the O_4 absorption cross-sections that are known to have large uncertainties (Wagner et al., 2002). Even at room temperature, the O_4 cross-sections reported in the literature (Greenblatt et al., 1990; Hermans et al., 1999) seem to provide an overestimation (up to 30 %) of the DSCD (Wagner et al., 2002, 2009; Clémer et al., 2010), but the magnitude of the correction to reconcile the models and measurements seems to be dependent on a number of factors. A case study was performed over Izaña on day number 204 at the O_4 477 nm band; a good correlation ($R^2 = 0.96$) was identified between the measurements and the RTM, which provides confidence in the magnitude of the retrieved optical paths. A similar result has been obtained recently by Baidar et al. (2013) using high-altitude aircraft measurements, which suggests that pressure, temperature or both play a role in the magnitude of the observed discrepancy. At our station, smaller O_4 cross-sections should be required to shift the measured O_3 concentrations towards the in situ values.

The differences between the MGA and in situ measurements may also be due to the different air masses scanned by each instrument. MAX-DOAS scans a FT area over the ocean far from the surface along a 60–70 km path. Therefore, the MAX-DOAS spectrometer provides the O_3 background in the FT. During summer, a subtropical high-pressure system induces subsidence that supplies high O_3 air masses from above, whereas at the observatory the effect is the opposite. A radiatively induced upslope breeze transports O_3-poor and NO_2-rich air from lower altitudes, which reduces the O_3 and increases the NO_2 mixing ratio recorded by the in situ instruments. As a result, the averaged differences between the hourly mean surface O_3 and the night-time background level can be as high as 20 ppbv on certain summer days (Cuevas et al., 2013). This is consistent with the fact that the larger differences between the MGA and in situ O_3 measurements appear when NO_2 in situ measurements are above their respective DL (50 pptv), see Fig. 9. In fact, these sudden increases of the in situ NO_2 concentration are a direct consequence of the MBE. Nevertheless, if the air transported by the breeze has a NO_2 mixing ratio lower than 50 pptv, the breeze might also exist but it will not be detected by the in situ NO_2 measurements. An example of this case was observed on day 205. Based in the in situ measurements performed prior to or after day 205, we can assume that, also on this day, the in situ recordings are affected by the MBE. Hence, this might explain the observed difference between the O_3 MGA and in situ measurements taken on day 205.

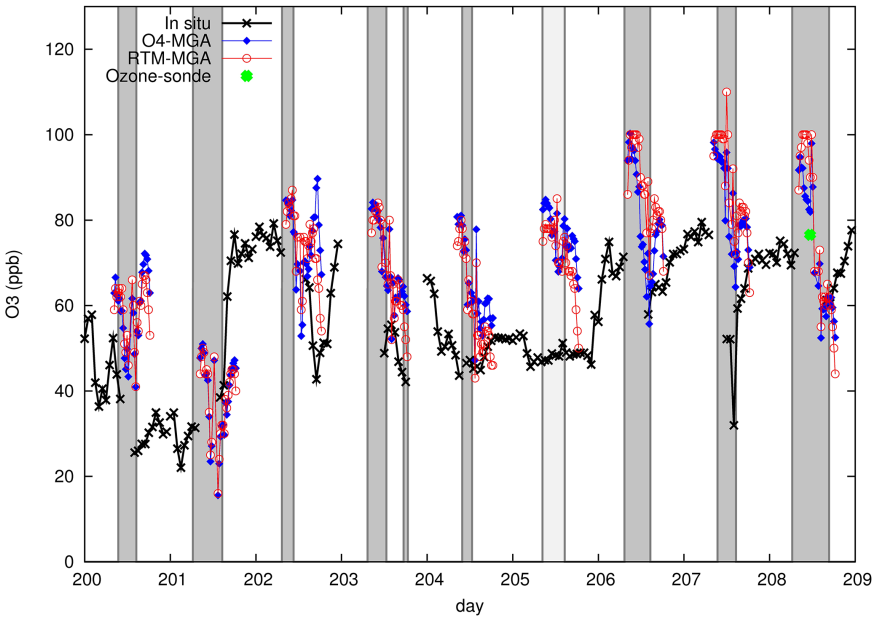

Figure 9. Surface O_3 mixing ratios (in ppbv) at the Izaña observatory. The red open circles correspond to the ozone mixing ratios obtained using single-scattering RTM-MGA. The blue diamonds correspond to O_3 mixing ratios obtained using O_4-MGA. The black crosses correspond to the in situ measurements. The green point corresponds to the O_3 concentration at the altitude of the station as obtained from the ozone-sounding. Dark grey regions correspond to those periods in which NO_2 in situ measurements are above the detection limit of the in situ instrument. Light grey indicates an increase in the in situ NO_2 measurements on day 205, below the detection limit.

The O_3 data at the level of the observatory measured by the ozone sounding launched on day 208 also supports this possibility (i.e. the different scanned air masses as the cause of the difference between MGA and in situ O_3 mixing ratios), see Fig. 9. Considering that the ECC.O_3 sonde accuracy in the troposphere is 8–10 % (Smit, 2011) ($\sim$ 8 ppbv on day 208 for an 80 ppbv mixing ratio at the level of the station), the O_3 value from the ozone-sonde at the Izaña level is in rather good agreement with the estimated MGA values. Note that during the study period (days 200–208), the in situ measurements end around noon for technical reasons. As a result, the MAX-DOAS and in situ measurements overlap only during some daylight hours. This could also be a cause of the observed differences between the MGA and in situ O_3 concentrations. To test this hypothesis, the mean diurnal O_3 volume mixing ratios for the RTM-MGA and in situ measurements were calculated. The daily averages for each instrument were calculated from two sets of data: all available data for each day and data for the periods of the day when simultaneous measurements were available. The results show that, when considering only simultaneous data, the differences between the MGA and in situ approach are not reduced, which eliminates the in situ noon blackouts as the cause of the discrepancy.

On some of the analysed days, the diurnal evolution of the O_3 concentration shows a decrease during the day that seems too large to be genuine. This is not observed for O_4 or NO_2, which suggests that the variation is not optical path related (i.e. azimuth changes). New experiments are in progress to identify the causes of this effect.

6.2 NO_2 concentration

The same procedure that was applied to O_3, was also used to obtain the NO_2 concentrations, but hourly profiles were calculated to account for photochemical changes. This allowed us to test the sensitivity of the retrieved concentration to the profile. The hourly profiles were obtained using a photochemical box model (Denis et al., 2005) derived from the SLIMCAT 3-D chemical transport model (Chipperfield, 2006).

In Fig. 10, the NO_2 results of RTM-MGA (red) are shown together with the in situ data (black). The O_4-MGA results are shown as blue diamonds. The NO_2 VRM are at the 20–30 pptv level. For such low NO_2 concentrations, no tools are available to decide which of the two retrievals is the most accurate. Nevertheless, the in situ NO_2 measurements are shown for reference because, during the night-time, the NO_2 concentrations are below the DL given by the manufacturer (50 ppt for the 300 s average).

Contrary to the observations of the O_3, the in situ NO_2 measurements increase to very high concentrations during the hours around noon. This increase is the result of the MBE. The mountain breeze brings anthropogenic NO_2, which originated over the populated areas of the coast, to the station. Thus, the mixing ratios increase to hundreds of ppt

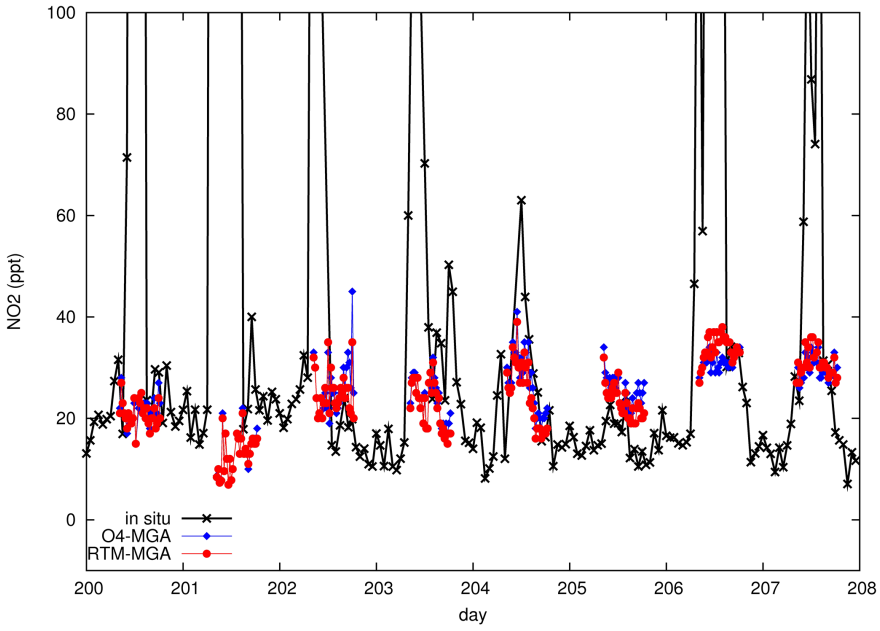

Figure 10. Surface NO_2 mixing ratios at the Izaña observatory for days 200 to 207. The black crosses correspond to the in situ measurements. The blue diamonds correspond to the NO_2 mixing ratios obtained with the O_4-MGA. The red solid circles correspond to the NO_2 mixing ratios obtained with the RTM-MGA.

around noon (Volz-Thomas et al., 1993; Puentedura et al., 2012). This local effect, which renders the in situ data non-representative of the FT during the daytime, is no more than a few hundred metres above the surface. The relative contribution of this narrow BML layer to the MAX-DOAS path is very low, and it is smoothed out in the long paths that were sampled. At night, a well-developed katabatic regime transports air masses from higher altitudes, which ensures that the measured NO_2 is representative of the FT conditions.

The NO_2 concentrations obtained from the MGA, as presented in this study, were also compared with previous FT NO_2 measurements obtained from research aircraft flights. Bucsela et al. (2008) measured NO_2 over the eastern Atlantic coast of North America during the Intercontinental Chemical Transport Experiment – North America, Phase A (INTEX-A), and the International Consortium for Atmospheric Research and Transformation (ICARTT) aircraft campaigns using the research DC-8 of NASA. These measurements were obtained using the UC Berkeley laser-induced fluorescence instrument (TD-LIF) whose DL is 4 ppt. These profiles reveal NO_2 concentration values that are similar to those found in this study (approximately 20 ppt) for the same altitude and the same time of the year (Martin et al., 2006; Bucsela et al., 2008).

7 Summary and conclusions

A new method, the MGA, was developed to obtain mixing ratios of trace gases in the FT. The MGA uses horizontal and near-zenith geometries to estimate a station level differential path. Two independent methods were used for the optical path calculation: the first method, O_4-MGA, uses MAX-DOAS SCDs of O_4; the second method, RTM-MGA, obtains optical paths from AMFs obtains optical paths from a RTM. The methodology is useful at high mountain observatories where horizontal measurements are possible and aerosol loading is low. The validity of the assumptions considered in this approximation and the applicability of this method have been confirmed for SZAs lower than 70°.

Both methods, O_4-MGA and RTM-MGA, were applied to MAX-DOAS measurements at the Izaña observatory to estimate FT O_3 and NO_2 mixing ratios. By comparing these results with in situ measurements, it is shown that under low aerosol loading, the mixing ratios of O_3 and NO_2 can be retrieved. Day-to-day O_3 variations are well captured by the MGA, although mean differences of 28 % between the MGA results and in situ measurements were observed. The different air masses that were scanned by each instrument are possible causes of these discrepancies. The NO_2 concentrations obtained with the MGA are within the range of 20–40 ppt, which is below the DL of the in situ chemiluminescent analyser but in good agreement with other subtropical FT measurements recorded by aircraft (Martin et al., 2006; Bucsela et al., 2008).

The main advantage of the MGA is that it provides mixing ratios that are only slightly affected by the MBE. Because air masses sampled by a MAX-DOAS spectrometer extend a few tens of kilometres, inhomogeneities are smoothed along the path. Therefore, unlike in situ data, MAX-DOAS

measurements are representative of the FT. Furthermore, the MGA provides a simple way to estimate O_3 mixing ratios when no in situ instruments are available. In fact, for NO_2, the method provides mixing ratios of a few tens of pptv, which are below the DL of the standard instrumentation based on chemiluminiscence.

Acknowledgements. Laura Gomez thanks the MINECO (Spanish Economy Ministry) for providing the *Juan de la Cierva* grant. We acknowledge the support of AMISOC (Atmospheric Minor Species relevant to the Ozone Chemistry at both sides of the Subtropical jet, contract number CGL2011-24891), and NORS (Demonstration Network of Ground-Based Remote Sensing Observations in support of the GMES Atmospheric Service) integrated project under the 7th Framework Programme (contract number FP7-SPACE-2011-284421). The authors thank Ramón Ramos and the CIAI staff for their support at the Izaña observatory and the Sieltec team for the instrument maintenance. We thank Philippe Goloub for his effort in establishing and maintaining the AERONET Izaña site.

Edited by: M. Van Roozendael

References

Anderson, G. P.: AFGL atmospheric constituent profiles (0–120 km), Hanscom AFB, MA: Optical Physics Division, Air Force Geophysics Laboratory, AFGL-TR; 86-0110, US Air Force Geophysics Laboratory, Optical Physics Division, 1986.

Baidar, S., Oetjen, H., Coburn, S., Dix, B., Ortega, I., Sinreich, R., and Volkamer, R.: The CU Airborne MAX-DOAS instrument: vertical profiling of aerosol extinction and trace gases, Atmos. Meas. Tech., 6, 719–739, doi:10.5194/amt-6-719-2013, 2013.

Beelen, R., Hoek, G., Pebesma, E., Vienneaud, D., Hoogh, K., and Briggs, D. J.: Mapping of background air pollution at a fine spatial scale across the European Union, Sci. Total Environ., 407, 1852–1867, doi:10.1016/j.scitotenv.2008.11.048, 2009.

Bogumil, K., Orphal, J., Flaud, J. M., and Burrows, J. P.: Vibrational progressions in the visible and near ultraviolet absorption spectrum of ozone, Chem. Phys. Lett., 349, 241–248, 2001.

Bucsela, E. J., Perring, A. E., Cohen, R. C., Boersma, K. F., Celarier, E. A., Gleason, J. F., Wening, M. O., Bertram, T. H., Wooldridge, P. J., Dirkisen, R., and Veefkind, J. P.: Comparison of tropospheric NO2 from in situ aircraft measurements with near-real-time and standard product data from OMI, J. Geophys. Res., 113, D16S31, doi:10.1029/2007JD008838, 2008.

Chipperfield, M. P.: New version of the TOMCAT/SLIMCAT off-line chemical transport model: Intercomparison of stratospheric tracer experiments, Q. J. R. Meteorol. Soc., 132, 1179–1203, doi:10.1256/qj.05.51, 2006.

Clémer, K., Van Roozendael, M., Fayt, C., Hendrick, F., Hermans, C., Pinardi, G., Spurr, R., Wang, P., and De Mazière, M.: Multiple wavelength retrieval of tropospheric aerosol optical properties from MAXDOAS measurements in Beijing, Atmos. Meas. Tech., 3, 863–878, doi:10.5194/amt-3-863-2010, 2010.

Cuevas, E., Díaz, A., and Martín, F.: Atmospheric Carbon Dioxide Concentration at Izaña BAPMoN Observatory, Canary Islands, 1984–1990, in: Proceedings 19th ITM on Air Pollution Modeling and its Applications, NATO/CCMS, Ierapetra, Greece, 29 September–4 October 1991, 45–46, edited by: van Dop, H. and Kallos, G., Plenum Press, New York, USA, 1992.

Cuevas, E., Lamb, K., and Bais, A.: Total Ozone Contents derived by Different Instruments and Soundings, Meteorological Publications No 27, Finnish Meteorological Institute, 105–119, Helsinki, 1994.

Cuevas, E., González, Y., Rodríguez, S., Guerra, J. C., Gómez-Peláez, A. J., Alonso-Pérez, S., Bustos, J., and Milford, C.: Assessment of atmospheric processes driving ozone variations in the subtropical North Atlantic free troposphere, Atmos. Chem. Phys., 13, 1973–1998, doi:10.5194/acp-13-1973-2013, 2013.

Dahlback, A. and Stamnes, K.: A new spherical model for computing the radiation field available for photolysis and heating at twilight, Planet. Space Sci., 39, 671–683, doi:10.1016/0032-0633(91)90061-E,1991.

Denis, L., Roscoe, H. K., Chipperfield, M. P., Van Roozendael, M., and Goutail, F.: A new software suite for NO_2 vertical profile retrieval from ground-based zenith-sky spectrometers, J. Quant. Spectrosc. Rad. Transf., 92, 321–333, doi:10.1016/j.jqsrt.2004.07.030, 2005.

Engardt, M., Bergström, R., and Andersson, C.: Climate and Emission Changes Contributing to Changes in Near-surface Ozone in Europe over the Coming Decades: Results from Model Studies, Ambio, 38, 452–458, 2009.

Fayt, C. and Van Roozendael, M.: WinDOAS 2.1. User Manual, IASB-BIRA, 2001.

Font, I.: El Tiempo Atmosférico de las Islas Canarias, Servicio Meteorológico Nacional (INM), Serie A, 26, 1956.

Frieß, U., Monks, P. S., Remedios, J. J., Rozanov, A., Sinreich, R., Wagner, T., and Platt, U.: MAX-DOAS O4 measurements: A new technique to derive information on atmospheric aerosols: 2. Modeling studies, J. Geophys. Res., 111, D14203, doi:10.1029/2005JD006618, 2006.

Gil, M., Yela, M., Gunn, L. N., Richter, A., Alonso, I., Chipperfield, M. P., Cuevas, E., Iglesias, J., Navarro, M., Puentedura, O., and Rodríguez, S.: NO_2 climatology in the northern subtropical region: diurnal, seasonal and interannual variability, Atmos. Chem. Phys., 8, 1635–1648, doi:10.5194/acp-8-1635-2008, 2008.

González, Y.: Levels and origin of reactive gases and their relationship with aerosols in the proximity of emission sources and in the free troposphere at Tenerife, PhD Thesis, Universidad de la Laguna (Canary islands, Spain), 2012.

Greenblatt, G. D., Orlando, J. J., Burkholder, J. B., and Ravishankara, A. R.: Absorption Measurements of Oxygen Between 330 and 1140 nm, J. Geophys. Res., 95, 18577–18582, 1990.

Hendrick, F., Müller, J.-F., Clémer, K., Wang, P., De Mazière, M., Fayt, C., Gielen, C., Hermans, C., Ma, J. Z., Pinardi, G., Stavrakou, T., Vlemmix, T., and Van Roozendael, M.: Four years of ground-based MAX-DOAS observations of HONO and NO_2 in the Beijing area, Atmos. Chem. Phys., 14, 765–781, doi:10.5194/acp-14-765-2014, 2014.

Hermans, C., Vandaele, A. C., Carleer, M., Fally, S., Colin, R., Jenouvrier, A., Coquart, B., and Mérienne, M. F., Absorption Cross-Sections of Atmospheric Constituents: NO_2, O_2 and H_2O, Environ. Sci. Poll. Res., 6, 151–158, doi:10.1007/BF02987620, 1999.

Hönninger, G. and Platt, U.: Observations of BrO and its vertical distribution during surface ozone depletion at Alert, Atmos. Environ., 36, 2481–2489, doi:10.1016/S1352-2310(02)00104-8, 2002.

Hönninger, G., von Friedeburg, C., and Platt, U.: Multi axis differential optical absorption spectroscopy (MAX-DOAS), Atmos. Chem. Phys., 4, 231–254, doi:10.5194/acp-4-231-2004, 2004.

Liang, O., Jaeglé, L., Jaffe, D. A., Weiss-Penzias, P., Heckman, A., and Snow, J. A.: Long-range transport of Asian pollution to the northeast Pacific: Seasonal variations and transport pathways of carbon monoxide, J. Geophys. Res., 109, D23S07, doi:10.1029/2003JD004402, 2004.

Ma, J. Z., Beirle, S., Jin, J. L., Shaiganfar, R., Yan, P., and Wagner, T.: Tropospheric NO_2 vertical column densities over Beijing: results of the first three years of ground-based MAX-DOAS measurements (2008–2011) and satellite validation, Atmos. Chem. Phys., 13, 1547–1567, doi:10.5194/acp-13-1547-2013, 2013.

Mahajan, A. S., Gómez Martín, J. C., Hay, T. D., Royer, S.-J., Yvon-Lewis, S., Liu, Y., Hu, L., Prados-Roman, C., Ordóñez, C., Plane, J. M. C., and Saiz-Lopez, A.: Latitudinal distribution of reactive iodine in the Eastern Pacific and its link to open ocean sources, Atmos. Chem. Phys., 12, 11609–11617, doi:10.5194/acp-12-11609-2012, 2012.

Mao, H., Talbot, R., Troop, D., Johnson, R., Businger, S., and Thompson, A. M.: Smart balloon observations over the North Atlantic: O_3 data analysis and modelling, J. Geophys. Res., 111, D23S56, doi:10.1029/2005JD006507, 2006.

Martin, R. V., Sioris, C. E., Chance, K., Ryerson, T. B., Bertram, T. H., Wooldridge, P. J., Cohen, R. C., Neuman, J. A., Swanson, A., and Flocke, F. M.: Evaluation of space-based constraints on global nitrogen oxide emissions with regional aircraft measurements over and downwind of eastern North America, J. Geophys. Res., 111, 5308, doi:10.1029/2005JD006680, 2006.

Mayer, B. and Kylling, A.: Technical note: The libRadtran software package for radiative transfer calculations – description and examples of use, Atmos. Chem. Phys., 5, 1855–1877, doi:10.5194/acp-5-1855-2005, 2005.

Melamed, M. L., Solomon, S., Daniel, J. S., Langford, A. O., Portmann, R. W., Ryerson, T. B., Nicks, D. K. J., and McKeen, S. A.: Measuring reactive nitrogen emissions from point sources using visible spectroscopy from aircraft, J. Environ. Monit., 5, 29–34, doi:10.1039/B204220G, 2003.

Milford, C., Marrero, C., Martin, C., Bustos, J. J., and Querol, X.: Forecasting the air pollution episode potential in the Canary Islands, Adv. Sci. Res., 2, 21–26, doi:10.5194/asr-2-21-2008, 2008.

Oltmans, S. J., Levy, H., Harris, J. M., Merrill, J. T., Moody, J. L., Lathrop, J. A., Cuevas, E., Trainer, M., O'Neill, M. S., Prospero, J. M., Vömel, H., and Jonson, B. J.: Summer and spring ozone profiles over the North Atlantic from ozonesonde measurements, J. Geophys. Res., 101, 29.179–29.200, doi:10.1029/96JD01713, 1996.

Palmén, E. and Newton, C. W.: Atmospheric Circulation Systems, International Geophysics Series, Vol. 13, Academic Press Ed., 603 pp., 1969.

Peters, E., Wittrock, F., Großmann, K., Frieß, U., Richter, A., and Burrows, J. P.: Formaldehyde and nitrogen dioxide over the remote western Pacific Ocean: SCIAMACHY and GOME-2 validation using ship-based MAX-DOAS observations, Atmos. Chem. Phys., 12, 11179–11197, doi:10.5194/acp-12-11179-2012, 2012.

Platt, U. and Stutz, J.: Differential Optical Absorption Spectroscopy: Principles and Applications, Springer-Verlag, Berlin, Germany, 2008.

Puentedura, O., Gil, M., Saiz-Lopez, A., Hay, T., Navarro-Comas, M., Gómez-Pelaez, A., Cuevas, E., Iglesias, J., and Gomez, L.: Iodine monoxide in the north subtropical free troposphere, Atmos. Chem. Phys., 12, 4909–4921, doi:10.5194/acp-12-4909-2012, 2012.

Reidmiller, D. R., Jaffe, D. A., Fischer, E. V., and Finley, B.: Nitrogen oxides in the boundary layer and free troposphere at the Mt. Bachelor Observatory, Atmos. Chem. Phys., 10, 6043–6062, doi:10.5194/acp-10-6043-2010, 2010.

Robinson, A. D., Millard, G. A., Danis, F., Guirlet, M., Harris, N. R. P., Lee, A. M., McIntyre, J. D., Pyle, J. A., Arvelius, J., Dagnesjo, S., Kirkwood, S., Nilsson, H., Toohey, D. W., Deshler, T., Goutail, F., Pommereau, J.-P., Elkins, J. W., Moore, F., Ray, E., Schmidt, U., Engel, A., and Müller, M.: Ozone loss derived from balloon-borne tracer measurements in the 1999/2000 Arctic winter, Atmos. Chem. Phys., 5, 1423–1436, doi:10.5194/acp-5-1423-2005, 2005.

Rodgers, C. D.: Inverse Methods for Atmospheric Sounding: Theory and Practice, vol. 2 of Atmospheric, Oceanic and Planetary Physics, World Scientific, Hackensack, NJ, doi:10.1142/9789812813718_fmatter, 2000.

Roscoe, H. K., Van Roozendael, M., Fayt, C., du Piesanie, A., Abuhassan, N., Adams, C., Akrami, M., Cede, A., Chong, J., Clémer, K., Friess, U., Gil Ojeda, M., Goutail, F., Graves, R., Griesfeller, A., Grossmann, K., Hemerijckx, G., Hendrick, F., Herman, J., Hermans, C., Irie, H., Johnston, P. V., Kanaya, Y., Kreher, K., Leigh, R., Merlaud, A., Mount, G. H., Navarro, M., Oetjen, H., Pazmino, A., Perez-Camacho, M., Peters, E., Pinardi, G., Puentedura, O., Richter, A., Schönhardt, A., Shaiganfar, R., Spinei, E., Strong, K., Takashima, H., Vlemmix, T., Vrekoussis, M., Wagner, T., Wittrock, F., Yela, M., Yilmaz, S., Boersma, F., Hains, J., Kroon, M., Piters, A., and Kim, Y. J.: Intercomparison of slant column measurements of NO_2 and O_4 by MAX-DOAS and zenith-sky UV and visible spectrometers, Atmos. Meas. Tech., 3, 1629–1646, doi:10.5194/amt-3-1629-2010, 2010.

Rothman, L. S., Gordon, I. E., Barbe, A., Benner, D. C., Bernath, P. F., Birk, M., Boudon, V., Brown, L. R., Campargue, A., Champion, J. P., Chance, K., Coudert, L. H., Danaj, V., Devi, V. M., Fally, S., Flaud, J. M., Gamache, R. R., Goldmanm, A., Jacquemart, D., Kleiner, I., Lacome, N., Lafferty, W. J., Mandin, J. Y., Massie, S. T., Mikhailenko, S. N., Miller, C. E., Moazzen-Ahmadi, N., Naumenko, O. V., Nikitin, A. V., Orphal, J., Perevalov, V. I., Perrin, A., Predoi-Cross, A., Rinsland, C. P., Rotger, M., Simecková, M., H.Smith, M. A., Sung, K., Tashkun, S. A., Tennyson, J., Toth, R. A., Vandaele, A. C., and VanderAuwera, J.: The HITRAN 2008 molecular spectroscopic database, available at: http://www.cfa.harvard.edu/hitran/updates.html#Watervaporupdate, J. Quant. Spectrosc. Rad. Transf., 110, 533–572, doi:10.1016/j.jqsrt.2009.02.013, 2008.

Sinreich, R., Frieß, U., Wagner, T., and Platt, U.: Multi axis differential optical absorption spectroscopy (MAX-DOAS) of gas and aerosol distributions, Faraday Discuss., 130, 153–164, doi:10.1039/b419274p, 2005.

Sinreich, R., Coburn, S., Dix, B., and Volkamer, R.: Ship-based detection of glyoxal over the remote tropical Pacific Ocean, Atmos. Chem. Phys., 10, 11359–11371, doi:10.5194/acp-10-11359-2010, 2010.

Sinreich, R., Merten, A., Molina, L., and Volkamer, R.: Parameterizing radiative transfer to convert MAX-DOAS dSCDs into near-surface box-averaged mixing ratios, Atmos. Meas. Tech., 6, 1521–1532, doi:10.5194/amt-6-1521-2013, 2013.

Smit, H. G.: Quality Assurance and Quality Control for Ozonesonde Measurements in GAW, Technical Report, World Meteorological Organization, Herman G. J. Smit and the Panel for the Assessment of Standard Operating Procedures for Ozonesondes (ASOPOS), 2011.

Solomon, S., Schmeltekopf, A. L., and Sanders, R. W.: On the interpretation of zenith sky absorption measurements, J. Geophys. Res. Atmos., 92, 8311–8319, 1987.

Steck, T.: Methods for determining regularization for atmospheric retrieval problems, Appl. Optics, 41, 1788–1797, doi:10.1364/AO.41.001788, 2002.

Stohl, A. and Trickl, T.: A textbook example of long-range transport: Simultaneous observation of ozone maxima of stratospheric and North American origin in the free troposphere over Europe, J. Geophys. Res., 104, 30445–30462, doi:10.1029/1999JD900803, 1999.

Stohl, A., Huntrieser, H., Richter, A., Beirle, S., Cooper, O. R., Eckhardt, S., Forster, C., James, P., Spichtinger, N., Wenig, M., Wagner, T., Burrows, J. P., and Platt, U.: Rapid intercontinental air pollution transport associated with a meteorological bomb, Atmos. Chem. Phys., 3, 969–985, doi:10.5194/acp-3-969-2003, 2003.

Thakur, A. N., Sing, H. B., Mariani, P., Chen, Y., Wang, Y., Jacob, D. J., Brasseur, G., Müller, J. F., and Lawrence M.: Distribution of reactive nitrogen species in the remote free troposphere: data and model comparison, Atmos. Environ., 33, 1403–1422, doi:10.1016/S1352-2310(98)00281-7, 1999.

Thompson, A. M., Oltmans, S. J., Tarasick, D. W., von der Gathen, P., Smit, H. G. J., and Witte, J. C.: Strategic ozone sounding networks: Review of design and accomplishments, Atmos. Environ., 45, 2145–2163, doi:10.1016/j.atmosenv.2010.05.002, 2011.

Vandaele, A. C., Hermans, C., Simon, P. C., Carleer, M., Colins, R., Fally, S., Mérienne, M. F., Jenouvrier, A., and Coquart, B.: Measurements of the NO_2 Absorption Cross-Sections from 42000 cm−1 to 10000 cm−1 (238–1000 nm) at 220 K and 294 K, J. Quant. Spectrosc. Rad. Transf., 59, 171–184, doi:10.1016/S0022-4073(97)00168-4, 1998.

Volz-Thomas, A., Schmitt, R., Cuevas, E., Prospero, J. M., Savoie, D., Graustein, W., and Turekian, K.: Concurrent Measurements of Carbon Monoxide, Ozone, NOy, PAN and Aerosols at Izaña, Tenerife. Atmospheric Chemistry of the North Atlantic and AEROCE II. A31g, 1993 Fall Meeting, American Geophysical Union, p. 145, 1993.

Wagner, T., von Friedeburg, C., Wening, M., Otten, C., and Platt, U., UV-Visible observations of atmospheric O4 absorptions using direct moonlight and zenith-scattered sunlight for clear-sky and cloudy sky conditions, J. Geophys. Res., 107, 4424, doi:10.1029/2001JD001026, 2002.

Wagner, T., Dix, B., v. Friedeburg, C., Frieß, U., Sanghavi, S., Sinreich, R., and Platt, U.: MAX-DOAS O4 measurements: A new technique to derive information on atmospheric aerosols – Principles and information content, J. Geophys. Res., 109, D22205, doi:10.1029/2004JD004904, 2004.

Wagner, T., Deutschmann, T., and Platt, U.: Determination of aerosol properties from MAX-DOAS observations of the Ring effect, Atmos. Meas. Tech., 2, 495–512, doi:10.5194/amt-2-495-2009, 2009.

Wenig, M., Spichtinger, N., Stohl, A., Held, G., Beirle, S., Wagner, T., Jähne, B., and Platt, U.: Intercontinental transport of nitrogen oxide pollution plumes, Atmos. Chem. Phys., 3, 387–393, doi:10.5194/acp-3-387-2003, 2003.

Zyryanov, D., Foret, G., Eremenko, M., Beekmann, M., Cammas, J.-P., D'Isidoro, M., Elbern, H., Flemming, J., Friese, E., Kioutsioutkis, I., Maurizi, A., Melas, D., Meleux, F., Menut, L., Moinat, P., Peuch, V.-H., Poupkou, A., Razinger, M., Schultz, M., Stein, O., Suttie, A. M., Valdebenito, A., Zerefos, C., Dufour, G., Bergametti, G., and Flaud, J.-M.: 3-D evaluation of tropospheric ozone simulations by an ensemble of regional Chemistry Transport Model, Atmos. Chem. Phys., 12, 3219–3240, doi:10.5194/acp-12-3219-2012, 2012.